

Clonality and allelotype analyses of focal nodular hyperplasia compared with hepatocellular adenoma and carcinoma

Yi-Ran Cai, Li Gong, Xiao-Ying Teng, Hong-Tu Zhang, Cheng-Feng Wang, Guo-Lian Wei, Lei Guo, Fang Ding, Zhi-Hua Liu, Qin-Jing Pan, Qin Su

Yi-Ran Cai, Xiao-Ying Teng, Hong-Tu Zhang, Guo-Lian Wei, Lei Guo, Qin-Jing Pan, Qin Su, Department of Pathology, Cancer Institute and Cancer Hospital, Chinese Academy of Medical Sciences and Peking Union Medical College, Panjiayuan Nanli 17, Beijing 100021, China

Li Gong, Department of Pathology, Tangdu Hospital, the Fourth Military Medical University, Xi'an 710038, Shaanxi Province, China

Cheng-Feng Wang, Department of Abdominal Surgery, Cancer Institute and Cancer Hospital, Chinese Academy of Medical Sciences and Peking Union Medical College, Beijing 100021, China

Fang Ding, Zhi-Hua Liu, State Key Laboratory of Molecular Oncology, Cancer Institute, Chinese Academy of Medical Sciences and Peking Union Medical College, Beijing 100021, China

Author contributions: Cai YR, Teng XY and Gong L performed the majority of experiments and participated in the manuscript preparation; Wei GL, Guo L and Ding F carried out some of the experiments; Wang CF, Liu ZH and Pan QJ provided valuable materials and performed data evaluation; Su Q designed the study and wrote the manuscript.

Supported by The National Natural Science Foundation of China (NSFC), Grants 30171052, 30572125 and 30772508 and the CAMS Cancer Hospital Clinical Research Project LC2007A21

Correspondence to: Qin Su, Professor, Department of Pathology, Cancer Institute and Cancer Hospital, Chinese Academy of Medical Sciences and Peking Union Medical College, Panjiayuan Nanli 17, Beijing 100021, China. q.su@wjgnet.com

Telephone: +86-10-87787508 Fax: +86-10-67713359

Received: July 7, 2009 Revised: August 17, 2009

Accepted: August 24, 2009

Published online: October 7, 2009

Abstract

AIM: To identify clonality and genetic alterations in focal nodular hyperplasia (FNH) and the nodules derived from it.

METHODS: Twelve FNH lesions were examined. Twelve hepatocellular adenomas (HCAs) and 22 hepatocellular carcinomas (HCCs) were used as references. Nodules of different types were identified and isolated from FNH by microdissection. An X-chromosome inactivation assay was employed to describe their clonality status. Loss of heterozygosity (LOH) was detected, using 57 markers, for genetic alterations.

RESULTS: Nodules of altered hepatocytes (NAH), the putative precursors of HCA and HCC, were found in all the FNH lesions. Polyclonality was revealed in 10 FNH lesions from female patients, and LOH was not detected in any of the six FNH lesions examined, the results apparently showing their polyclonal nature. In contrast, monoclonality was demonstrated in all the eight HCAs and in four of the HCCs from females, and allelic imbalances were found in the HCAs (9/9) and HCCs (15/18), with chromosomal arms 11p, 13q and 17p affected in the former, and 6q, 8p, 11p, 16q and 17p affected in the latter lesions in high frequencies ($\geq 30\%$). Monoclonality was revealed in 21 (40%) of the 52 microdissected NAH, but was not found in any of the five ordinary nodules. LOH was found in all of the 13 NAH tested, being highly frequent at six loci on 8p, 11p, 13q and 17p.

CONCLUSION: FNH, as a whole, is polyclonal, but some of the NAH lesions derived from it are already neoplastic and harbor similar allelic imbalances as HCAs.

© 2009 The WJG Press and Baishideng. All rights reserved.

Key words: Clonality analysis; Focal nodular hyperplasia; Hepatocellular adenoma; Liver tumorigenesis; Loss of heterozygosity; Nodules of altered hepatocytes

Peer reviewer: Toru Ishikawa, MD, Department of Gastroenterology, Saiseikai Niigata Second Hospital, Teraji 280-7, Niigata, Niigata 950-1104, Japan

Cai YR, Gong L, Teng XY, Zhang HT, Wang CF, Wei GL, Guo L, Ding F, Liu ZH, Pan QJ, Su Q. Clonality and allelotype analyses of focal nodular hyperplasia compared with hepatocellular adenoma and carcinoma. *World J Gastroenterol* 2009; 15(37): 4695-4708 Available from: URL: <http://www.wjgnet.com/1007-9327/15/4695.asp> DOI: <http://dx.doi.org/10.3748/wjg.15.4695>

INTRODUCTION

Focal nodular hyperplasia (FNH) is defined as a lesion composed of hyperplastic hepatic parenchyma, subdivided into nodules by fibrous septa that may form stellate scars^[1,2]. As dystrophic vessels are observed in

the fibrous septa and an arteriole is present within most of the nodules, it is considered parenchyma overgrowth responsive to increased blood flow secondary to vascular malformations^[3]. Morphologically, FNH is classified into two categories, classical and nonclassical lesions^[4]. The latter includes telangiectatic, mixed hyperplastic/adenomatous types and lesions with cytologic atypia. The non-neoplastic nature appears to be supported by data from X-chromosome inactivation (XCI) analyses, which demonstrated polyclonality in all FNH lesions in most of the series^[5,6]. However, monoclonality was also observed in some of the lesions^[7], including telangiectatic FNH^[8,9]. FNH, as a descriptive term when proposed^[10], may represent a group of focal lesions with different morphologic phenotypes and genetic alterations, and may develop in different pathways. Chromosomal gains and losses have been observed in several lesions by comparative genomic hybridization, allelotyping or karyotyping^[9,11], but the molecular mechanism of FNH development remains unclear.

Hepatocellular adenoma (HCA) is a benign hepatic neoplasm, and its development is associated with the long-term use of steroids, mainly oral contraceptives^[2,12]. While HCA was proven to develop from foci of altered hepatocytes (FAH) in the liver of rodents^[13], the neoplastic features of human HCA have been confirmed by clonality analyses^[5,6,9]. Some HCA lesions tend to progress to hepatocellular carcinoma (HCC)^[2,13], and the malignant transformation has been linked to β -catenin activation^[14]. In contrast to HCA, FNH is a stable lesion in clinical phenotypes with a very low risk of malignant transformation, although FAH can be detected in FNH^[15] and HCC was identified in the liver harboring FNH as described in several case reports^[16-18].

The majority of FNH lesions are distinguishable from HCA by their morphologic features. However, the differential diagnosis is difficult for some lesions. A central scar is regarded as the most characteristic change, but it is detectable in less than half of FNH lesions. Even for classical FNH, its incidence was shown to be 62% (153/245)^[4,19]. More reliable procedures remain to be established for its distinction from HCA.

In the present study, we examined the clonality status of FNH, and compared its clonality with that of HCAs and HCCs, using assays based on XCI and polymorphism at the androgen receptor (AR) and phosphoglycerate kinase (PGK) loci. Secondly, these lesions were examined for loss of heterozygosity (LOH). In addition, 57 nodules were microdissected from FNH in female patients and used for the clonality analysis. Twenty-five nodules were also isolated from an FNH lesion and were used for LOH analysis.

MATERIALS AND METHODS

Tissue samples and histological examination

A total of 46 hepatic lesions were used, including 12 FNH lesions from 10 patients (Table 1), 12 HCAs from 11 patients and 22 well-differentiated HCCs (Table 2).

These patients were admitted to the Cancer Hospital, Chinese Academy of Medical Sciences in Beijing and Tangdu Hospital, the Fourth Military Medical University in Xi'an during the period from 1998 to 2007. All the lesions were resected by an operation. Representative formalin-fixed, paraffin-embedded tissue samples were retrieved from the archives for both tumors and the surrounding liver parenchyma. Sections of 4 μ m in thickness were prepared and stained by hematoxylin and eosin (HE).

All slides were reexamined independently by three pathologists (Su Q, Cai YR and Gong L), and their histologic features were reevaluated. FNH of the classical form was considered when the lesions showed characteristic features as proposed by other authors^[3,4,10]. All the HCA lesions were identified from livers without evidence of cirrhosis or diffuse fibrosis by their macroscopical and histological features using well-established criteria^[2]. FAH and nodules of altered hepatocytes (NAH) were identified on HE-stained sections^[20], and the lesions were further highlighted by a marked reduction or even absence of CK18-immunoreactivity in glycogenotic clear cells as described previously^[21]. Dysplasia, also designated as "small-cell change (SCC)"^[20,22] and "small-cell dysplasia"^[23], was recognized and graded into low-grade and high-grade lesions. The histological grades of HCCs were assessed as described by Hamilton and Aaltonen^[11], with the well-differentiated HCCs corresponding to all of the grade I and some of the grade II lesions by the criteria of Edmondson and Steiner^[24].

Immunohistochemical staining was performed using a streptavidin-labeled peroxidase (S-P) kit as in our previous study^[20]. The primary antibodies used in this study included those against cytokeratin (CK) 18, CK19, CD34, hepatitis B virus (HBV) surface antigen (HBsAg; Clone 3E7), p53 protein (DO-7) and Ki-67 antigen. All reagents were purchased from Dako (Glostrup, Denmark). Levels of Ki-67 antigen expression were expressed as Ki-67-labeling indices (Ki-67-LI). The nuclear accumulation of p53 protein was evaluated as many (3+, > 30%), moderate (2+, 5%-30%), few (+, < 5%) and absent (-, 0%), as described previously^[25].

Extraction of genomic DNA

Sections of 8 μ m in thickness were prepared. After staining with HE, the lesions of FNH, HCA and HCC were identified by microscopic examination. Then the lesional tissues, each covering an area of at least 1 cm \times 1 cm, were collected by a rubber policeman, and pooled into 1.5-mL tubes. The surrounding liver parenchyma and fibrous tissue were collected and used as controls. Previous XCI tests have demonstrated that monoclonality can be determined provided a given cell population contains at least 75% monoclonal cells^[26]. To guarantee reliability of the following assays, mesenchymal tissue areas containing inflammatory cell clusters were eliminated to enhance purity of target cells to at least 80%. Genomic DNA was then isolated with

Table 1 Clinicopathological features of 12 FNH lesions and data of immunohistochemistry, clonality and LOH assays

| Case numbers | Age (yr)/gender | Lesion codes | Lesion sizes (cm) | Ki-67-LI (%) | p53-LI (%) | Clonality by XCIA | No. of LOH |
|--------------|-----------------|-------------------|-------------------|--------------|------------|-------------------|------------|
| 01 | 40/F | 01 ¹ | 5.0 | 1.6 | 0 | PC ² | 0 |
| 02 | 30/F | 02 | 2.5 | 0.5 | 0 | PC ² | 0 |
| | | 03 | 7.0 | 0.8 | 0 | PC ² | 0 |
| 03 | 22/M | 04 ³ | 5.2 | 0.7 | 0 | NT | 0 |
| 04 | 44/M | 05 ¹ | 1.2 | 0.5 | 0 | NT | 0 |
| 05 | 31/F | 06 ¹ | 4.7 | 0.3 | 0 | PC ² | 0 |
| 06 | 43/F | 07 | 3.2 | 1.0 | 0 | PC ² | NT |
| 07 | 44/F | 08 ¹ | 2.0 | 0.8 | 0 | PC ⁴ | NT |
| 08 | 53/F | 09 ⁵ | 4.8 | 1.0 | 0 | PC ² | NT |
| 09 | 23/F | 10 ^{1,5} | 4.5 | 1.2 | 0 | PC ⁴ | NT |
| 10 | 46/F | 11 ^{1,5} | 5.3 | 0.8 | 0 | PC ³ | NT |
| | | 12 ¹ | 1.5 | 0.9 | 0 | PC ⁴ | NT |

¹Some small preneoplastic foci, composed of clear cells, identified in surrounding liver parenchyma; ²Tested on phosphoglycerate kinase (PGK) locus; ³Nodules of altered hepatocytes (NAH) isolated from FNH by microdissection for LOH detection; ⁴Noninformative at PGK locus and the data obtained by the assay on androgen receptor (AR) locus; ⁵NAH isolated from FNH by microdissection for clonality assessment by XCIA. FNH: Focal nodular hyperplasia; Ki-67-LI: Ki-67 antigen-labeling indices; p53-LI: p53 protein-labeling indices by DO-7; XCIA: X-chromosomal inactivation assay; LOH: Loss of heterozygosity; F: Female; M: male; PC: Polyclonality; NT: Not tested for its origin from a male patient.

Table 2 Clinicopathological features of 12 HCAs and 22 HCCs, with data of clonality and LOH assays

| Case numbers | Age (yr)/gender | Lesion codes | Lesion sizes (cm) | Lesion types | Ki-67-LI (%) | p53-LI (%) | Clonality by XCIA | No. of LOH | Chromosomal arms affected by LOH |
|--------------|-----------------|--------------|-------------------|-----------------------|--------------|------------|-------------------|------------|----------------------------------|
| 11 | 36/F | HCA01 | 3.5 | HCA | 1.3 | 0 | MC ¹ | 3 | 8p, 11p, 16q |
| 12 | 57/F | HCA02 | 3.0 | HCA ² | 1.3 | 0 | MC ¹ | 1 | 17p |
| 13 | 28/M | HCA03 | 7.3 | HCA, SCC ² | 2.5 | 0 | NT | 4 | 11p, 13q, 17p |
| 14 | 52/M | HCA04 | 8.5 | HCA | 1.1 | 0 | NT | 3 | 11p, 17p |
| 15 | 31/F | HCA05 | 7.0 | HCA | 3.1 | 0 | MC ¹ | 4 | 11p, 13q |
| 16 | 29/F | HCA06 | 1.0 | HCA ² | 2.0 | 0 | MC ¹ | NT | NT |
| | | HCA07 | 12.0 | HCA ² | 1.8 | 0 | MC ¹ | 5 | 1p, 13q, 17p |
| 17 | 30/F | HCA08 | 1.0 | HCA, SCC ² | 1.5 | 0 | MC ³ | 1 | 13q |
| 18 | 29/F | HCA09 | 5.0 | HCA | 0.9 | 0 | MC ¹ | 4 | 6q, 11p, 13q, 17p |
| 19 | 37/F | HCA10 | 5.0 | HCA | 1.3 | 0 | MC ³ | 2 | 13q, 17p |
| 20 | 33/F | HCA11 | 2.0 | HCA ² | 2.3 | 0 | MC ¹ | NT | NT |
| 21 | 40/F | HCA12 | 1.5 | HCA ² | 2.0 | 0 | MC ³ | NT | NT |
| 22 | 31/F | HCC01 | 2.2 | HCC, G1 | 2.0 | 10 | NT | 11 | 8p, 11p, 13q, 16q, 17p |
| 23 | 46/M | HCC02 | 4.1 | HCC, G1 | 65.0 | 0 | NT | 7 | 6q, 13q, 16q, 17p |
| 24 | 42/M | HCC03 | 3.0 | HCC, G1 | 2.5 | 0 | NT | 10 | 6q, 8p, 13q, 17p |
| 25 | 51/M | HCC04 | 5.3 | HCC, G1 | 8.2 | 80 | NT | 5 | 8p, 11p, 13q, 16q, 17p |
| 26 | 49/M | HCC05 | 2.0 | HCC, G1 | 2.0 | 0 | NT | 2 | 1p, 11p |
| 27 | 27/M | HCC06 | 2.5 | HCC, G1 | 1.2 | 0 | NT | 2 | 8p, 11p |
| 28 | 56/M | HCC07 | 3.3 | HCC, G1 | 1.5 | 0 | NT | 0 | None |
| 29 | 38/F | HCC08 | 8.3 | HCC, G1 | 18.0 | 0 | MC ¹ | NT | NT |
| 30 | 64/F | HCC09 | 3.6 | HCC, G1 | 5.5 | 0 | MC ³ | NT | NT |
| 31 | 53/F | HCC10 | 9.5 | HCC, G2 | 8.5 | 0 | NT | 3 | 8p |
| 32 | 33/M | HCC11 | 8.0 | HCC, G2 | 5.2 | 0 | NT | 5 | 6q, 11p, 17p |
| 33 | 48/F | HCC12 | 5.2 | HCC, G2 | 35.0 | 0 | NT | 4 | 6q, 8p, 16q |
| 34 | 44/F | HCC13 | 4.2 | HCC, G2 | 65.0 | 80 | NT | 12 | 8p, 11p, 13q, 16q, 17p |
| 35 | 29/F | HCC14 | 3.6 | HCC, G2 | 0.9 | 0 | NT | 2 | 1p, 11p |
| 36 | 61/F | HCC15 | 4.5 | HCC, G2 | 3.7 | 0 | NT | 6 | 6q, 13q, 16q, 17p |
| 37 | 48/M | HCC16 | 5.0 | HCC, G2 | 1.4 | 0 | NT | 3 | 6q, 11p, 17p |
| 38 | 39/M | HCC17 | 4.0 | HCC, G2 | 1.5 | 0 | NT | 0 | None |
| 39 | 39/M | HCC18 | 5.0 | HCC, G2 | 1.2 | 0 | NT | 0 | None |
| 40 | 50/M | HCC19 | 2.0 | HCC, G2 | 2.0 | 0 | NT | 8 | 8p, 11p, 13q, 17p |
| 41 | 51/M | HCC20 | 7.4 | HCC, G2 | 12.2 | 0 | NT | 1 | 11p |
| 42 | 55/F | HCC21 | 2.5 | HCC, G2 | 28.5 | 0 | MC ³ | NT | NT |
| 43 | 77/F | HCC22 | 5.6 | HCC, G2 | 16.2 | 0 | MC ³ | NT | NT |

¹Noninformative at PGK locus and the data obtained by the assay on AR locus; ²Some small preneoplastic foci, composed of clear cells, identified in surrounding liver parenchyma; ³Tested on PGK locus. HCA: Hepatocellular adenoma; HCC: Hepatocellular carcinoma; MC: Monoclonality; NT: Not tested for its origin from a male patient (for HCA) or its evidently malignant phenotypes; SCC: Small-cell change.

an extraction kit (QIAGEN, Chatsworth, CA, USA) following the manufacturer's instructions. The DNA samples of 50 μ L each were stored at -20°C until use.

Microdissection of preneoplastic nodules from FNH

Selected FNH specimens with well demarcated NAH were subjected to microdissection as described previously¹²⁷.

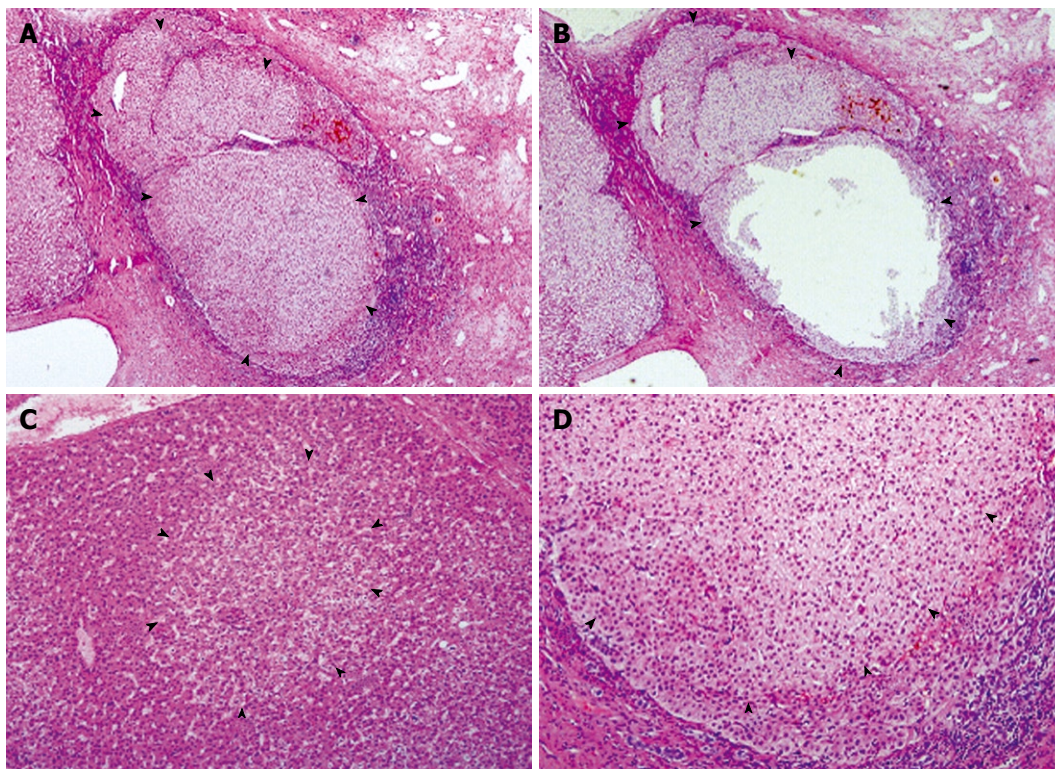


Figure 1 Premeoplastic lesions in classical FNH. A and B: FNH04 from Case 03, showing a nodule largely occupied by an expanding NAH (arrowheads), before (A) and after microdissection (B); C: Portion of FNH06, showing an FAH (arrowheads), in which the altered hepatocytes integrate well with the surrounding hepatic plate; D: Portion of an NAH composed mainly of clear hepatocytes (arrowheads), showing compression to surrounding liver parenchyma. HE, A and B, $\times 40$; C and D, $\times 100$.

Ten consecutive sections were deparaffinized with xylene, rehydrated by rinsing through graded alcohol, stained with HE and immersed in glycerol. Larger nodules, 2.5-5.0 mm in diameter, from these sections were identified and correlated. Target tissues were outlined and collected with a clean $4\frac{1}{2}$ needle under a microscope (Figure 1A and B). The tissues of the same nodules from the consecutive sections were pooled together and stored in 1.5-mL tubes. Using the same procedure, tissues of the same size were also collected from the surrounding liver parenchyma and were used as controls. Genomic DNA was isolated as described above.

Clonality assays based on XCI mosaicism in somatic tissues in female patients

The principles of XCI assays have been described previously^[28]. Briefly, there are two X chromosomes within each somatic cell in females, one from the father and the other from the mother. Both PGK and AR genes are located on X chromosomes, showing readily demonstrable polymorphism in different frequencies. The former carries a *Bst*XI restriction-polymorphic site, reflecting the G/A single-nucleotide polymorphism at exon 1, while the latter is polymorphic at the CAG short tandem repeat (STR). These allelic differences and the XCI mosaicism enable us to identify monoclonal, neoplastic lesions from normal or regenerating tissues composed of polyclonal cell populations^[28,29].

The DNA templates extracted from tumors and the non-neoplastic tissues were incubated with 5 U of *Hpa*II (Promega, Madison, WI, USA) at 37°C for 12 h in a volume

of 20 μ L containing 0.2 μ L of 10 mg/mL bovine serum albumin and 2 μ L of 10 \times reaction buffer, and heated at 95°C for 5 min to inactivate the enzyme. The digested DNA samples, 5 μ L each, were then subjected to nested PCR for amplification of exon 1 of PGK and AR genes, as described previously^[28]. The PGK products, 10 μ L each, were incubated with 5 U of *Bst*XI (Promega) at 47°C for 8-10 h. The digested products were then resolved in 2% (g/mL) agarose gel containing ethidium bromide (0.2 μ g/mL), and visualized under ultraviolet light. The fluorescence intensities of the products of these two alleles, at the positions of 530 and 433 bp separately, were assessed using LabWork 3.0 (UVP). Efficacy of the reaction was demonstrated by including a sample from a male patient with FNH (Case 03) who had been demonstrated to harbor a *Bst*XI restriction site.

The amplification products of AR exon 1, 3 μ L each, were mixed with the same volume of sample buffer (99% formamide, 1 mg/mL bromophenol blue, 1 mg/mL xylene cyanol), resolved on 10% polyacrylamide gel containing urea (8.0 mol/L), and visualized by silver staining. Sizes of the products were determined using 100-bp and 10-bp DNA ladders (Gibco BRL).

LOH assays by conventional and multiplex PCR

A total of 57 loci, whose allelic loss has been frequently observed in HCC samples from various regions^[30-38], were chosen for the LOH assay. Amplification of the DNA samples from the whole FNH lesions, HCAs and HCCs was performed by conventional PCR. Sequences of the primer pairs (Table 3) were obtained from Genbank

Table 3 Sequences of primers for nested PCR-based LOH assays

| Markers (locations) | External primer pairs ¹ | Internal primer pairs ¹ |
|---------------------|---|---|
| D1S199 (1p36.13) | CCTGGGCAACATAGCAG TGACATCTTCTCCACCTC | GGTGACAGAGTGAGACCCCTG CAAAGACCATGTGCTCCGTA |
| D1S2843 (1p36.12) | AGAAGGTCGGGCACAAA TTCATCACCCACCCAAAA | GGGCTGGGCATTACACAAC ATCAAATGGCTTCTCACCG |
| D1S513 (1p35.2) | AGCTGAGACCCTGCCTTG AATGCCTGCTGATGAAA | AGCTGAGACCCTGCCTTG AGCCTTCAGAGCCTGCC |
| D4S406 (4q31.21) | TCCCAGTTTACAACCACA GAAGGTGGCTAACTAAAA | CTGGTTTTAAGGCATGTTTG TCCTCAGGGAGGTCTAAT |
| D4S426 (4q35.2) | CAAGTAATACAATATGGTAA ATACACTGCATCCATATATACAAGG | ATACACTGCATCCATATATACAAGG ACATTGTGAAATGACCACAG |
| D6S437 (6q25.3) | TTACTGACTTCTTGAAGGGTG ACACGCCATCACAGGAAC | TGTCCTGGTGGAGGCA GGTACAGTGTGTTGACCCTAAGA |
| D6S305 (6q26) | AAAGCTGAGAAGCCATTCA GCAAATGGAGCATGTCACT | CACCAGCGTTAGAGACTGC GCAAATGGAGCATGTCACT |
| D6S1008 (6q27) | GCTACTTCAGCAGGGTT AATGACCACGAGTCTTTC | AAGAAAGACTAGAGAGACAGACAGC ATCATTGGCCATTTACCAA |
| D6S297 (6q27) | CAAGAAGTGTCTCTAAAGATAAGG GCAAGATGTAGAAGGAGA | CAAGAAGTGTCTCTAAAGATAAGG CAACCAACCACGGTATATG |
| D8S277 (8p23.1) | GTTCCCTATGGCTAAAG AGTTTGCCTCCAGAAA | CCAGGTGAGTTTATCAATTCCTGAG TGAGAGGTCTGAGTGACATCCG |
| D8S1754 (8p22) | TTTGGGTAAGATACTTTAAGCG AAATAGTCGGGTCGGGAG | CAGGGAAAGTCTCGGTTTG TCAGGGACACGATTACAGC |
| D8S1827 (8p22) | AGAAAATAGCCAAAGAAAGC CTGGGAAGGTCAGCAGATTG | GACAGAATCATGTGGCCTTT TTTTGTAAAATGTAAAATGGCTTT |
| D8S261 (8p22) | GAGGCTACTAACCAACGTG TATTACAGTGGTTATGGC | TGCCACTGCTTGAAAATCC TATGGCCCAGCAATGTGTAT |
| D8S258 (8p21.3) | ACAATAATGATGAGGCCAGAA CAGCCAATACGCAGGAGC | CTGCCAGGAATCAACTGAG TTGACAGGGACCCACG |
| D8S298 (8p21.3) | CTAGTTATTATGCAGAGGTGACATC GAGGCTGGTTAGCATCAG | AGGCTTACACCCATGGACC ACGCAGCACACAACATCAT |
| D8S1771 (8p21.2) | GGGGTGGGTGIAGATATT TTGATTCCTTGTGATGC | TTTACAAGAACCACCTGCC GATATAAAAACATGACTTTGTACCC |
| D8S1772 (8q22.1) | TTGATGCTCCCTGTGTTGC AAGTCCCTCCCTTTGCTGA | GATCTGAGCCTTCTACTGIC TGCCCTTTGGTGAATGG |
| D8S522 (8q24.12) | TATAGCAAATATGTTCAAG CCATCTTGGCTCCTC | GAAAACAAAACAGGCTCC TGACCAAACAACCTAGCACCC |
| D11S1301 (11p13) | GCCACAGCACTCCAG GACAACCTCCCTCACC | GGCAACAGAGTGAGACTCA GTGTTCCTTATGTGTAGTTC |
| D11S2008 (11p13) | ATTCAGGAGCACAGAACA GCATCCATACGAAAAGTC | CATCCATCTCATCCCATCAT TTCACCCTACTGCCAACTTC |
| D11S907 (11p13) | GCTTATTGTCCATACCCAAA GAAAAGCAAAGGCATCGT | GCTTATTGTCCATACCCAAA AAAGNACCTTAATTTACGGC |
| D13S164 (13q12.3) | GGCGATCCACCCACCTT TGCCACGCACCTGTAGTCC | GCTGTGATTGCACCACC ATTACAGGCGTGACACACC |
| D13S289 (13q12.3) | AGGGCGTCACCGTGT GACTGAGGCAGGAGGATTG | CTGGTTGAGCGGCATT TGCAGCCTGGATGACA |
| D13S260 (13q12.3) | AATGGATCTGCTTGC ATCACTCCAATGTAAAT | AGATATTGCTCCCGTCCATGA CCCAGATATAAGGACCTGGCTA |
| D13S171 (13q12.3) | CAGATACAGACATTTGGAA GCTCTACAGCATTGACCT | CCTACCATTGACACTCTCAG TAGGGCCATCCATTCT |
| D13S267 (13q13.1) | AGCTAATGGCCTGAAAAGG AGAGGTCAAAGAGGAAGA | GGCCTGAAAAGGTATCCTC TCCCACCATAAGCACAAG |
| D13S220 (13q13.2) | AATCACCTCCCACCAG AGGGGTTCTTCATCC | CCAACATCGGGAACCTG TGCATTCCTTAAGTCCATGTC |
| D13S219 (13q13.3) | CTGGATGAAAAGGAAC TTATCTCATTCAAGTGTCT | AAGCAAATATGAAAATTTGC TCCTTCTGTTCTTGACTTAACA |
| D13S218 (13q13.3) | TTCTCATAAGAAATCCCC TTTCATATCCCTGTTCAA | GATTTGAAAATGAGCAGTCC GTCGGGCACTACGTTTATCT |
| D13S325 (13q14.11) | ATGCAGCTTAAGTCTTT CTGTGCTATCTCCTCAA | TCCTTTAAGTGTCTAGAGAGGAGG TCTCTCTCAGAAGTTTGAAGC |
| D13S291 (13q14.11) | GTCTGACGGGAAACAGC CACAAACAGAATCAACCCT | ATGGCCAGACTTCCCCT CCAGGCTCACATGCTAACA |
| D13S126 (13q14.2) | AGCTCCCAAAGTGCTA AGTCAICTGGTCCCTCAAT | TCACCAGTAAAATGCTATTGG GTGATTTTCAAATTTGCTCTG |
| D13S118 (13q14.2) | TGTAATAGCTTAGTTG CTACTGACATTGCTC | GAAAATAGTATTTGGACCTGGG CCACAGACATCAGAGTCCCT |
| D13S153 (13q14.2) | AACTTGGCTGCGATGATAAGAA CCTGAGGTATTGACGAAGGGTC | AGCATTGTTTCATGTTGGTG CAGCAGTGAAGGTCTAAGCC |
| D13S284 (13q14.3) | CCAGCTCGTGTTCATTT | AAAATCAGGTGGAACAGAAT |

| | | |
|-----------------------------|---|---|
| D13S137 (13q14.3) | GTACATTTTATAGATTCATAGAGTIC GATGGIGGGTGGGACTIT | AAAGGCTAACATCGAAGGGA CAGGAGGGATGGACTCACTTC |
| D13S321 (13q21.1) | GGAATATGTGGAGGATTTATCTCTG TAAATGCAATCTGAAT | TTTCCTCATTCTTCCCAATTG TACCAACATGTTTCATGTAGATAGA |
| D13S119 (13q21.1) | CATAGCAAGACTCIGTC TCTCATTTCCATAACAT | CATACACCTGTGGACCCATC TTATTGCCTTTGTAGATCATTG |
| D13S170 (13q31.1) | 5' AGAGGAAAGATAGAACAA AGCIATTATGTAACCAAT | AAGACTTTGAATGAAATTCCC TTGCACTGTGGAGATAAACACATAG |
| D13S71 (13q31.3) | TGTTGTTCTAAGCCAC ACGCCTCTCGTGGIG | TCACATGTCTTTTAAAGCGAGGAG GTATTTTGGTATGCTTGTGC |
| D16S514 (16q21) | GTCCTCTGTTTCTCCTATT TGACACGCAATTTACCCT | CTATTTTGGAAATATATGTGCCT CTATCCACTCACTTTCCAGG |
| D16S402 (16q22.1) | AATCACATTTTCCACTG GAGGCAAAGAGGTATCCA | TCCCACGTACATCTTCIC TTTTGTAACCATGTACCCCC |
| D16S3029 (16q23.1) | CCCCTCATTCTGTCCC AGGGTGTGAGGTGTCTG | ATTTATAGGGCCATGACCAG ATAGAGTTGGGCTGCATAGA |
| D16S3040 (16q23.2) | ATAGGGTCTGCTGGGTT TATGTTGGTGGATGATT | CFTTCTGAAATTTGGAAGTGA TACTCCGGCAAGGACG |
| D16S422 (16q24.3) | 5' GTCAAGGAACTGAACT ACAGCCACCCTATTCA | GCTGCCTAGCACATGG CAGTGTAACCTGGGGG |
| D16S3121 (16q24.3) | AACATTTACTATATCTTACTTTCC AAGTCACTGGGCTAACCAAGG | CTTTCCGATTAGTTAGCAGAATGAG CATGTTGTACATCTGATGC |
| D16S303 (16q24.3) | TGGTCTCTGAGGTACAAA GCAGTTATGGATGIGAGTTTGT | AGCTTTTATTTCCAGGGGT GATCAGTGTCTGTTTTTTTGGTTTGG |
| D17S643 (17p13.3) | TTCCGAAGGCTGAGGCACTA TGCCGTTCTCAGGTGGTT | CAACAAGAGCGGAACTCGGTCTCAA CTTCTTGTCTCTAAACAGTCCITT |
| D17S849 (17p13.3) | TTCCTCCCTGCATGGATT TACAATACTGCTGCAATAAG | GTAGTCCCAGGGAGCTGGAAGT CAATTCGTCTAAGATTATTTTGG |
| D17S926 (17p13.3) | TACAATAACATCAGGAAACA GAAGTGGGAAGATTGCTT | CCTGGCTGAGGAGGC GCAGTGGCCATCATCA |
| D17S695 (17p13.3) | ATCCTCTGAACCGTATTT AGCCTGGGCAACAAGAGC | CCGAGAAGGCTGTGT CTGGGCAACAAGAGCAAAATTC |
| D17S1840 (17p13.3) | CAGCCAACGGGCGTCATT GGCAACGTGGTGAACCC | TTGTGTTGTTCATTGACTTCAGTCT GCCTGGGCGACAGATGA |
| D17S1529 (17p13.3) | ACCAGGACCGGCTCTCT GTTAGCCTCTTCTTGGACATTC | TGGGCAGACTTGGTCTT TTGTTTCTATCCACGAGGC |
| D17S1574 (17p13.3) | ATCATTCCGTTTACCTTTGG CTTCTCTGCGTCAGGTATG | GATGGCTGTGCTTGTCTGGTA TACTTATCGGCATCTGATCC |
| D17S831 (17p13.3) | CCAAAGTGCTGGGATTA GCCCAAATCAGAAGCAAG | CTGATGTGCCTTTTGTGTGTG CGCCTTCTCATACTCCAG |
| D17S654 (17p13.3) | GACATCCATTGGCACCAC GGGTACGCCTTCTCTCA | GCCAGACGGGACTGAAITA GACCTAGGCCATGTTACAGCC |
| D17S796 (17p13.2) | GGTTGGCAAGACCCTGTTAGA GAGCAGTAGGATCAAGGG | GACATCCATTGGCACCACCCCAA CAATGGAACCAAAATGTGGTC |
| β -actin ² | AGAACGGCAAACAACGAA CTGTGCCATCTACGAGG | AGTCCGATAATGCCAGGATG AGAGATGGCCACGGCTGCIT |
| | AAAGGGTGTAAACGCACTAA | ATTTGCGGTGGACGATGGAG |

¹Nucleotide sequences were written in a 5' to 3' direction, with the forward and reverse primers for each reaction presented at the upper and lower lines, respectively; ²Amplified as an internal control with a product of 406 bp.

(<http://www.ncbi.nlm.nih.gov> and www.gdb.org). The reaction mixture was 50 μ L in volume, containing 50 ng of DNA templates, 4 μ L of dNTP (2.5 mmol/L each; Gibco BRL), 1 μ L of 20 μ mol/L primers each, 5 μ L of 10 \times buffer (100 mmol/L Tris-HCl, pH 8.3, containing 500 mmol/L KCl and 25 mmol/L MgCl₂) and 1.25 U of *Taq* DNA polymerase (Gibco BRL). Amplification was conducted for 35 cycles (94°C, 40 s; 46°C, 50 s; 72°C, 1 min) following the initial denaturation at 94°C for 5 min. The final elongation was at 72°C for 15 min. The efficacy and reliability of the reactions were ensured by amplification of the β -actin gene in a parallel reaction.

For microdissected samples, the amounts of DNA extracted from the minute tissues were too small to complete all the reactions, and a highly efficient amplification system was needed. Nested PCR was employed for this purpose. A multiplex PCR was performed, according to

the principle of Henegariu *et al*^[39], followed by a second-round reaction in separate tubes. For the first-round PCR, 57 external primer pairs, as listed in Table 3, were designed based on the genomic sequences (Genbank). They were classified into 11 groups according to calculated annealing temperatures and compatibility with the assistance of Beacon Designer (Version 5.0) software, allowing amplification of four to seven STR sequences in the same mixture. The reaction mixture was 50 μ L in volume as described above, but it contained 20 ng of DNA templates. The amplification was performed for 35 cycles, and the annealing temperatures varied according to the primer groups. The second-round amplification was followed using the internal primer pairs (Table 3), with the 57 reactions in separate tubes. After initial denaturation at 94°C for 5 min, amplification was conducted for 15 cycles (94°C, 40 s; 50°C, 50 s; 72°C, 1 min) at first,

followed by 25 cycles with the annealing temperature adjusted to 46°C. The amplification products, 3 µL each, were mixed with the same volume of sample buffer, and then electrophoresed on a 15% polyacrylamide gel containing urea (8 mol/L). Gels were fixed in 10% acetic acid for 30 min, and the resolved products were visualized by silver staining.

Evaluation of data and statistical analyses

The images of the gels were subjected to analysis with a densitometer (Applied Syngene, Cambridge, UK). For clonality analysis based on polymorphism at the PGK and AR loci, a reduction of $\geq 50\%$ in their signal intensities for the products of either allele, as compared to the samples not treated with *Hpa*II or *Hba*I, is regarded as loss of XCI mosaicism^[28]. Each reaction was repeated at least once to guarantee reproducibility. Moreover, parallel assays were carried out using the surrounding liver parenchyma or fibrous tissue as controls. For the tests on microdissected lesions, special attention was paid to avoid interference from the XCI skewing patches^[28]. For each FNH lesion, four tissue samples of similar sizes as microdissected nodules were taken from the surrounding liver parenchyma and examined as controls.

For the heterozygosity test, normal tissue samples showing signals from two alleles migrating at expected locations and with similar intensities were considered informative, and those showing only one signal, were considered noninformative. Allelic imbalance was determined by comparing the intensity ratio between the signals for the two alleles. For a given informative marker, LOH was identified when one of two signals was absent or the allelic ratio was greater than 3 or less than 0.33. Reliability of the assays was guaranteed by including control tissue samples for all FNH lesions and microdissected nodules in a parallel way. Interpretation of LOH results of the lesions was considered reasonable when all of the control reactions from the same case gave rise to consistent allelic ratios.

Statistical computation was carried out using SPSS 13.0 software (SPSS, Inc, Chicago, IL, USA). Student and Kruskal-Wallis tests were employed to assess cell kinetic features of different lesion types reflected by Ki-67-LI, and the χ^2 test was used to compare LOH frequencies in HCA, FNH and HCC groups. $P < 0.05$ was regarded as statistically significant.

RESULTS

Clinical and pathological features

Twelve FNH lesions (FNH 01-12) were identified from 10 patients (Cases 01-10), eight patients had solitary lesions and separate lesions were identified in two liver specimens (Table 1). The patients included eight females and two males, aged 22-53 years (mean, 37.6 years). Grossly, the resected FNH lesions were 1.2-7.0 cm in diameter (mean, 3.8 cm), and were invariably described as circumscribed and solid lesions. On cut surfaces, a

multinodular appearance was observed, and a fibrous stellate scar was not recorded in any of the lesions. Histologically, all the lesions were classified as the classical form^[4], being well demarcated from the surrounding liver parenchyma but free of a fibrotic capsule. The lesions were subdivided incompletely into nodules with fibrous septa that contained malformed blood vessels, proliferating ductules, and scattered lymphocytes.

Most of the hepatocyte nodules appeared similar, about 1-5 mm in diameter, and histologically resembling regenerative nodules from cirrhotic livers. FAH, frequently of the clear cell type and clear/amphophilic mixed cell type, were identified in some of the nodules from all the lesions. The altered hepatocytes were arranged in plates frequently of two cells in thickness, with the sinusoids appearing crowded, but were integrated well with the surrounding hepatocytes in the majority of the lesions (Figure 1C). In some nodules, nearly all the parenchymal cells were replaced by the altered hepatocytes. These lesions became larger than other nodules, 2.5-5 mm in diameter, showing marked compression to the surrounding tissue (Figure 1D) and fulfilling the criteria for NAH^[20,22]. In all the FNH lesions, including the FAH and NAH areas, the thickness of hepatic plates did not exceed two cells and no SCC was detected. All the lesions were negative for p53 protein. Ki-67-LI ranged from 0.3% to 1.6%, with a mean of 0.8%. While this value was shown to be lower than those of HCAs ($P < 0.01$) and the well-differentiated HCCs ($P < 0.01$), these three lesion types showed overlap in their Ki-67-LI, with 6 (50%) of the 12 HCAs and 6 (27%) of the 22 HCCs within the range of FNH (Tables 1 and 2). FAH, mainly small-sized, and clear-cell lesions, were also identified in the surrounding liver parenchyma in six of the 10 livers (Table 1).

As listed in Table 2, 12 HCAs (HCAs 01-12) were resected from 11 patients (Cases 11-21), including nine females and two males. The ages of the patients ranged from 28 to 57 years (mean, 36.6 years), and none had a history of using oral contraceptives or other steroid hormones. Among the 12 lesions, 10 were solitary, and two were resected from the same liver (Case 16). The lesions ranged in size from 1 to 12 cm in diameter (mean, 4.8 cm). Histologically, the lesions were well demarcated from the surrounding liver parenchyma, but an intact fibrotic capsule was absent in all the lesions. The tumor was composed of hepatocytes arranged in plates usually of two cells in thickness. Low-grade SCC was identified in HCAs 03 and 08. The portal tract was not visible within the lesions. All these lesions were negative for p53 protein. Ki-67-LI ranged from 0.9% to 3.1%, with a mean of 1.8%. Phenotypic change of the sinusoid cells, as highlighted by emergence of CD34-immunoreactivity, was observed in all the HCA lesions, being diffuse in four and patchy in eight of the lesions. FAH, mainly of the clear cell type, were also identified in the surrounding liver parenchyma in six of the 11 livers.

A total of 22 well-differentiated HCCs were collected from 12 males and 10 females (Table 2). The age of the patients ranged from 27 to 77 years, with a mean of

Table 4 Nonrandom X-chromosomal inactivation revealed in NAH microdissected from 3 FNH and their inactivation patterns

| Origin of lesions | No. of NAH tested | No. with signals | No. with MC (%) | No. of lesions with | |
|-------------------|-------------------|------------------|-----------------|---------------------|------------|
| | | | | Upper band | Lower band |
| FNH09 | 38 | 34 | 14 (41.2) | 12 | 2 |
| FNH10 | 6 | 6 | 2 (33.3) | 0 | 2 |
| FNH11 | 12 | 12 | 5 (41.7) | 0 | 5 |
| Total | 56 | 52 | 21 (40.4) | 12 | 9 |

46.6 years. All the patients were shown to be seropositive for HBsAg. Of the 22 HCC cases, 20 appeared solitary and well demarcated and two were multifocal. The lesions ranged in size from 2.0 to 9.5 cm, with a mean of 4.6 cm. Histologically, nine of them were classified into grade 1, and 13 into grade 2. Ki-67-LI ranged from 0.9% to 65%, with the mean and median being 13.1% and 5.4%, respectively. This value was shown to be higher than that of HCAs ($P < 0.05$), while the Ki-67-LI in 10 (45%) of the 22 HCCs were within the range of HCAs. Immunoreactivity for AFP was demonstrated in four of the HCC samples (HCC 01, 11, 21 and 22). Overexpression of p53 protein was observed only in three HCC lesions, with the percentages of positive tumor cells as high as 10% in Case 21 and 80% in Cases 25 and 34. HBV infection was confirmed by immunohistochemical demonstration of HBsAg in all of the cases. Cirrhotic changes were evident in surrounding liver tissues in all the cases, where numerous NAH were identified.

Nonrandom XCI revealed in HCCs and HCAs, but not in the FNH lesions

XCI analysis was performed using tissues from 4 of the female patients with HCC (Cases 29, 30, 42 and 43) and all the nine females with HCA (Table 2). The G/A polymorphism at the PGK locus was demonstrated in three of the HCC patients (Cases 30, 42 and 43) and in three of the nine HCA patients (Cases 17, 19 and 21), showing two bands at positions 530 and 433 bp. Pretreatment with *Hpa*II resulted in loss, or marked intensity reduction, of one band in all the tumor samples, while the allelic ratio was retained in the samples from surrounding liver parenchyma (Figure 2A). One HCC (Case 29) and the remaining HCA patients were not polymorphic at the PGK locus, but the AR locus showed CAG STR length-polymorphism. Pretreatment with *Hha*I resulted in loss, or marked intensity reduction, of one band in these two tumor samples, while the allelic ratios were not changed in the corresponding peritumorous liver parenchyma (Figure 2B and C). These results demonstrated monoclonality and confirmed neoplastic nature in all the HCC and HCA lesions.

Of the eight female patients with FNH, 5 (Cases 1, 2, 5, 6 and 8) showed G/A polymorphism at the PGK locus, and the remaining three (Cases 7, 9 and 10) were shown to be AR-polymorphic at the CAG STR. Pretreatment with *Hpa*II (for PGK locus) or *Hha*I (for AR locus) did not cause a remarkable allelic ratio change in any of the 10 FNH samples (Figure 3A). These results demonstrated polyclonality of classical FNH lesions.

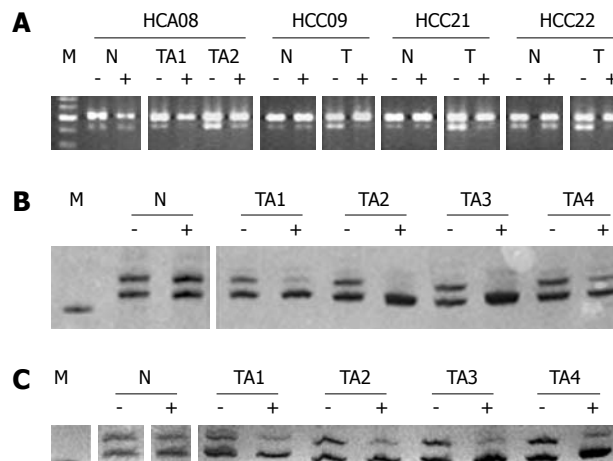


Figure 2 Representative data of X-chromosome inactivation (XCI) assays at PGK (A) and AR loci (B and C). Nonrandom XCI are present in HCAs (08 in A, 20 in B) and HCCs (09, 21 and 22 in A, 08 in C), revealing their monoclonality. A: The G/A single-nucleotide polymorphism at PGK exon 1 was demonstrated by *Bst*XI-digestion and electrophoresis on an agarose gel. The intact and cleaved amplification products migrate at positions of 530 (upper band) and 433 bp (lower band), respectively. Pretreatment with *Hpa*II (-: Before; +: After) resulted in marked reduction of the lower band in single tumor samples (T) and separate tumor areas (TA), but not in the surrounding liver parenchyma (N). M: DNA markers, with five bands at locations of 700, 600, 500, 400 and 300 bp; B and C: The length polymorphism of AR gene was resolved on a 10% polyacrylamide gel containing urea (8 mol/L) and visualized by silver staining, with one product migrating faster than the other. Pretreatment with *Hha*I (-: Before; +: After) resulted in loss or marked reduction of one band in tumor samples, but not in the non-neoplastic tissue. M: DNA marker at the location of 200 bp.

It appears that FNH is different in clonal composition from hepatocellular neoplasms including HCC and HCA.

Nonrandom XCI revealed in some NAH lesions microdissected from FNH

Three FNH lesions (FNH 09-11) with well-demarcated NAH from three women were chosen for microdissection. A total of 56 NAH lesions (NAH 01-56), ranging from 2.5 to 5 mm in diameter, and 5 ordinary regenerative nodules, of similar sizes and without involvement of FAH, were isolated from the FNH lesions for clonality analysis. Genomic DNA samples from 52 of the 56 dissected NAH were amplified successfully and subjected to AR (FNH 09 and 10) and PGK gene analysis (FNH11). Twenty-one (40%) of the 52 NAH showed monoclonality, including 14 (41%) of the 34 lesions in FNH09 (Figure 3B), 2 (33%) of the six in FNH10 and 5 (42%) of the 12 from FNH11 (Table 4). On average, the cross sectional areas of the 21 mono-

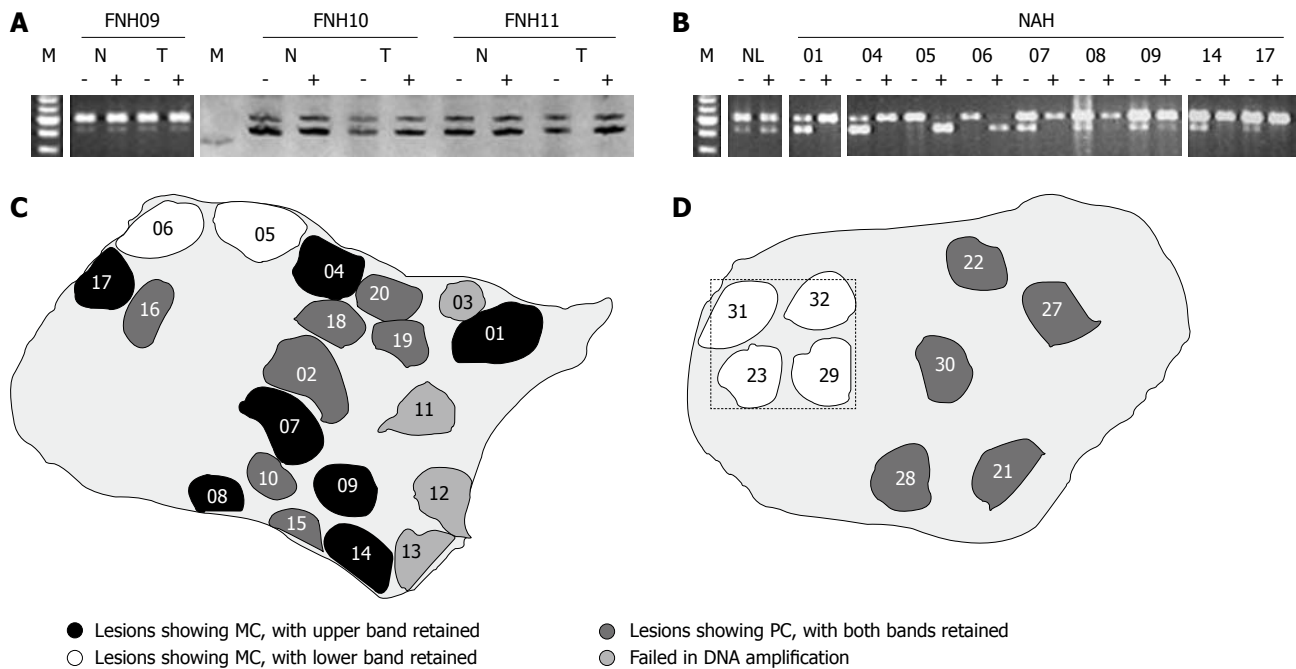


Figure 3 Clonality status of FNH lesions (A) and NAH (B), with XCI patterns revealed in different NAH (C and D). A: Polyclonality (PC) revealed in 3 FNH lesions, with FNH09 assayed at PGK locus and 10 and 11 at AR locus. *Hpa*II or *Hha*I pretreatment (-: Before; +: After) did not significantly change intensity ratios between the two bands of lesional tissues (T) compared to those of the surrounding liver parenchyma (N). M: DNA markers, with five bands at locations of 700, 600, 500, 400 and 300 bp for PGK assay, and a single band at the location of 200 bp for AR reaction; B: The PGK assay shows mono-clonality (MC) in all of the nine NAH from FNH09, with the isolated reference tissue sample (NL), of a similar size to NAH, revealing polyclonality. XCI patterns of the NAH are different, with the upper band retained in NAH 01, 04, 07-09, 14 and 17, and the lower band retained in NAH 05 and 06; C: Sketch of a tissue section from FNH09, as illustrated in B, showing occurrence of mono-clonal NAH with different XCI patterns and polyclonal lesions in the same section; D: Sketch of a tissue section from FNH11, showing four mono-clonal and five polyclonal NAH. The clustered mono-clonal lesions show the same XCI pattern, the XCI assays with small samples, as framed by hatch lines, may result in misinterpretation as mono-clonality for the whole FNH lesion.

and 31 polyclonal lesions were 9.8 ± 7.0 and 9.5 ± 6.7 mm², respectively, the difference being insignificant ($P > 0.05$). Different alleles were retained among the 14 mono-clonal NAH from FNH09 (Figure 3B and C), while identical inactivation patterns were observed in those NAH from FNH 10 and 11 (Figure 3D). All of the five ordinary nodules, four dissected from FNH09 and one from FNH11, were shown to be polyclonal in cell composition.

LOH detected in NAH, HCAs and HCCs, but not in whole FNH lesions

A total of 57 loci were examined in this study, located at 1p, 4q, 6q, 8p, 8q, 11p, 13q, 16q and 17p (Table 3). As shown in Table 2, the assay showed LOH, at least at one of the loci, in 15 (83%) of the 18 well-differentiated HCCs (01-07 and 10-20) and in all of the 9 HCAs examined (01-05 and 07-10, Figure 4A). Six of the FNH lesions (01-06), covering areas of at least 1.0 cm × 1.0 cm, were also examined, and no LOH was detected in any of them (Figure 4B).

Demonstration of clonal growth in some of the NAH from FNH, as described above, indicated that some genomic alterations may have occurred in these minute lesions. Twenty-five NAH were microdissected from an FNH lesion (FNH04) for LOH analysis. Genomic DNA samples from 13 of the microdissected lesions (NAH 57-69) were amplified successfully for the majority of the reactions, but for other samples

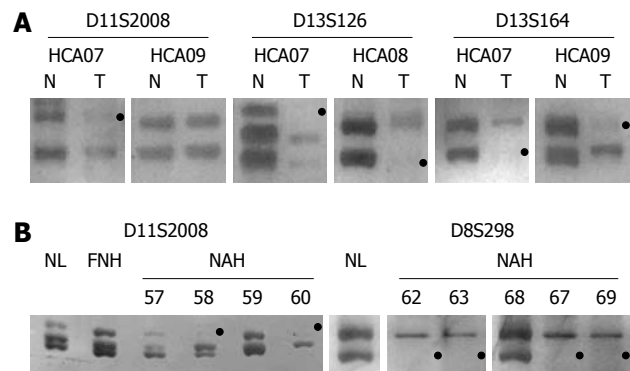


Figure 4 Representative data of amplification products at three length-polymorphic loci in HCAs 07-09 (A), FNH04 and NAH microdissected from the FNH lesion (B), with loss or marked reduction of the product from one allele (black dot) defined as LOH. A: Gels show the allelic imbalance at D11S2008, D13S164 and D13S164 in HCA07, at D13S126 in HCA08, at D13S164, but not in D11S2008, in HCA09 (T: Tumor; N: Peritumorous normal liver); B: The microdissected lesions NAH58 and NAH60, but not NAH57 and NAH59, show LOH at D11S2008. The lesions NAH62, NAH63, NAH67 and NAH69, but not NAH68, show LOH at D8S298. Both alleles are preserved in FNH04 as tested as a whole (FNH) and compared to those of the surrounding normal liver parenchyma (NL).

(NAH 70-81), the amounts of the extracted DNA were too small to complete all the reactions and the data obtained were not included. Allelic imbalance, at least at one of the loci, was demonstrated in all of the 13 NAH (Figure 4B, Table 5). The reliability of the assay was confirmed by full consistency between the results

Table 5 LOH profiles of 13 NAH microdissected from an FNH lesion (FNH04)

| Lesion codes | Diameters (mm) ¹ | Numbers of LOH | Loci affected ² |
|--------------|-----------------------------|----------------|---|
| NAH57 | 3.8 | 6 | D6S437, <u>D8S298</u> , <u>D13S118</u> , D13S153, D16S3029, D16S3040 |
| NAH58 | 3.5 | 5 | <u>D8S298</u> , <u>D11S1301</u> , D11S2008, <u>D13S321</u> , D16S3121 |
| NAH59 | 1.8 | 2 | <u>D13S164</u> , <u>D17S1840</u> |
| NAH60 | 2.7 | 2 | <u>D11S1301</u> , <u>D13S321</u> |
| NAH61 | 3.8 | 6 | D11S2008, <u>D13S118</u> |
| NAH62 | 3.2 | 4 | <u>D8S298</u> , <u>D13S164</u> , <u>D13S321</u> , <u>D17S1840</u> |
| NAH63 | 2.8 | 5 | D1S513, <u>D8S298</u> , <u>D13S118</u> , D13S153, D17S695 |
| NAH64 | 3.8 | 5 | D6S1008, D13S218, D16S514, D16S3040, D17S926 |
| NAH65 | 3.2 | 5 | D1S513, <u>D8S298</u> , D11S907, <u>D13S164</u> , D13S126 |
| NAH66 | 2.0 | 1 | D6S1008 |
| NAH67 | 2.1 | 4 | <u>D8S298</u> , <u>D11S1301</u> , D11S907, D16S422 |
| NAH68 | 2.4 | 3 | <u>D13S164</u> , D13S126, <u>D13S321</u> |
| NAH69 | 2.8 | 5 | D6S437, <u>D8S298</u> , D13S118, <u>D13S321</u> , D17S926 |

¹The largest diameters as measured in cross sections of the lesions under a microscope; ²The markers written in underlined characters represent loci affected in high frequencies ($\geq 30\%$) in NAH.

obtained by the multiplex reactions and those obtained through conventional PCR.

Of the 57 loci examined, 39 (68.4%) showed LOH in at least one of the lesions tested. At the remaining loci, allelic imbalance was not detected in any of the samples examined. LOH was demonstrated in NAH, HCAs and HCCs at 21 (37%), 16 (28%) and 33 loci (58%), respectively. The allelic imbalance was more extensive among the locations tested in HCCs than in HCAs and NAH ($P < 0.01$), with their average numbers of LOH being 4.5 (0-12), 3.1 (1-5) and 4.1 (1-6), respectively. As shown in Figure 5, the most frequent LOH in NAH, HCA and HCC were at D8S298 (70%), D11S1301 (75%) and D6S1008 (50%), respectively. Several markers showed frequent LOH in the HCC samples but not in HCAs, including D6S1008, D8S1754, D8S261, D8S277, D16S3029, D16S303 and D17S796.

While LOH was demonstrated in NAH, HCAs and HCCs, its frequencies were found to vary with locations in the genome and lesion types (Figure 5), with those up to 20% and 30% considered frequent and highly frequent events, respectively. Of the 39 loci showing LOH, eight were found to be highly frequent in HCAs, clustering at 11p, 13q and 17p, six in the HCCs, located at 6q, 8p, 11p, 16q and 17p, and six in NAH, located at 8p, 11p, 13q and 17p.

Differences between these types of lesions were further demonstrated by their LOH frequencies at different locations at 8p, 11p and 17p (Figure 5). Among the four loci affected at 8p, D8S298 was the only one showing LOH in a high frequency (70%) in NAH. Its frequencies were lower in other clinically detectable hepatocellular neoplasms, being 20% in HCAs and 12% in the HCC samples. The difference between NAH and HCC was significant ($P < 0.01$), and that between NAH and HCAs did not reach statistical significance ($P > 0.05$). Among the three loci at 11p, D11S1301 and D11S2008 were affected more frequently in NAH, HCA and HCC.

As shown in Figure 5, allelic imbalances were found to affect more chromosomal locations in HCC specimens, with LOH demonstrated preferentially at D8S261 (3/8, 38%), D8S1754 (4/13, 31%), D8S277 (3/15, 20%) and

D17S796 (38%). Among the loci, D17S796 did not show allelic imbalance in any of the six NAH and 10 HCAs examined. The region 17p13.3, as shown using nine markers, was affected in 7 (39%) of the 18 HCCs, 6 (67%) of the nine HCAs and 6 (46%) of the 13 NAH examined, with the locus D17S926 involved frequently in all of the three lesions. The region 16q21-24, as tested using seven markers, was affected in 6 (33%) of the 18 HCCs, 1 (11%) of the nine HCAs and 5 (38%) of the 13 NAH examined, with D16S3029 and D16S3040 affected frequently in HCC and NAH, but not in HCA specimens.

DISCUSSION

FNH occurs within an otherwise normal liver, and is detected more frequently between the ages of 20 and 50 years. A careful survey of 168 patients in France revealed a marked female predominance, with the male to female ratio being 1/8 (18/150)^[4]. However, a male predilection was observed in a report from China involving 86 FNH cases, with the male to female ratio being 1.7:1 (54:32)^[19]. This may reflect the differences in lifestyle and eco-environmental factors between these two countries, as a similar tendency has also been noticed for HCA^[6]. The role of oral contraceptive use in its development remains a matter of debate^[40,41], while its progression was observed in women using oral contraceptives^[42-44]. The lesion is frequently solitary. A minority of cases ranging from 7% (6/86)^[19] to 24% (40/168)^[4] have been shown to have multiple (2 to 30) lesions.

The distinction between FNH and HCA may be difficult in some cases during pathological practice. A central stellate scar, when present, is helpful in establishing the diagnosis of FNH. However, this feature is undetectable in about half of FNH lesions^[4,19]. Moreover, a similar change was also observed in some well-differentiated HCCs^[45]. In our study, this hallmark feature was not recorded in any of the 12 lesions examined. Clearly, more reliable approaches are needed for the differential diagnosis.

The pathogenesis of FNH remains to be established. Wanless and collaborators proposed that FNH is a

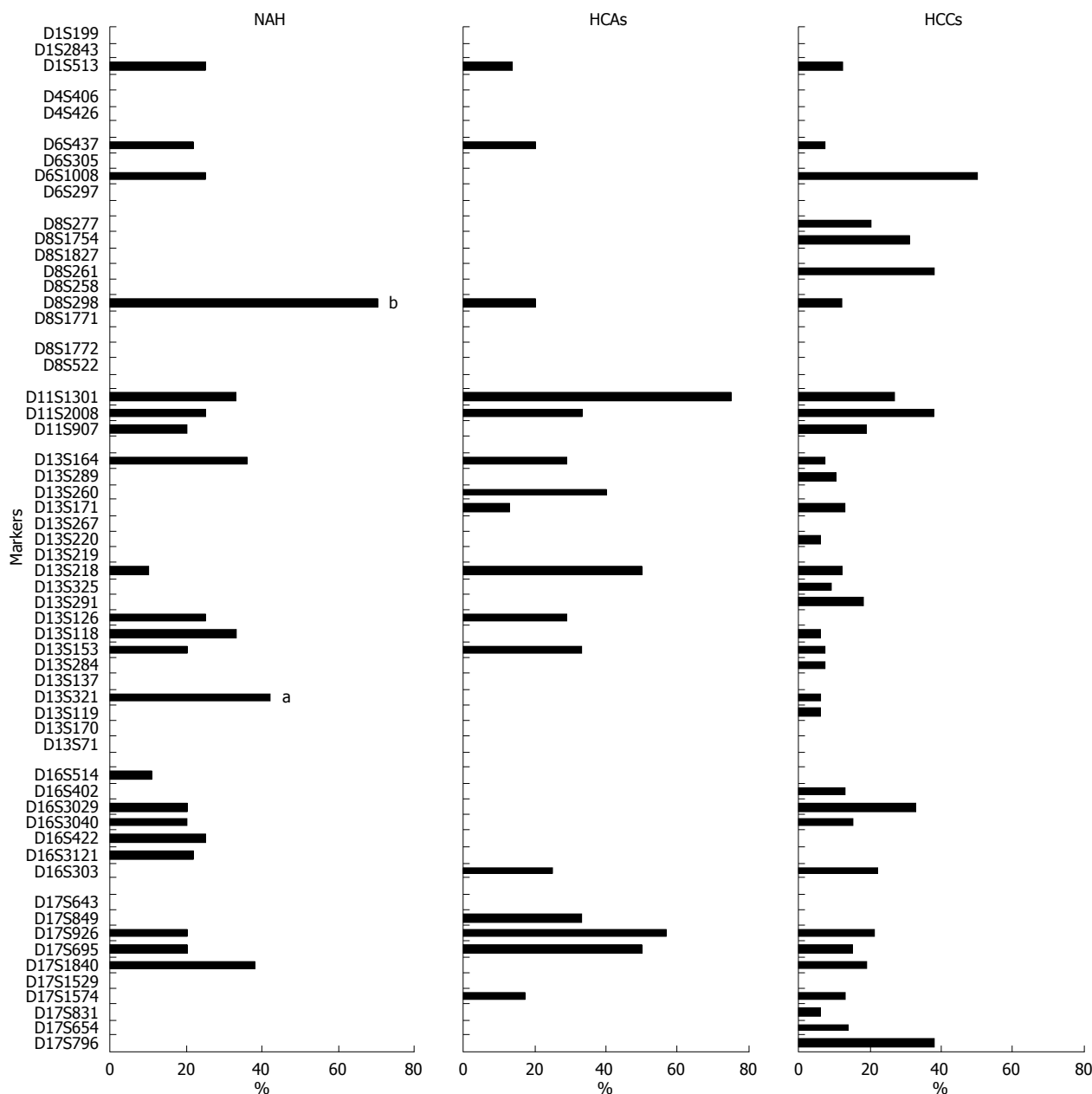


Figure 5 Frequencies of LOH as demonstrated using 57 microsatellite markers in NAH (n = 13), HCAs (n = 9) and well-differentiated HCCs (n = 18). ^aP < 0.05, ^bP < 0.01 vs HCCs.

proliferative response to an arterial malformation^[3]. Analysis of angiopoietin (ANGPT) 1 and ANGPT2 mRNA expression revealed an increase in the ANGPT1/ANGPT2 ratio in classical FNH, but not in HCA and telangiectatic FNH^[8,9,46]. This may provide a possible mechanism for alterations in proliferation and remodeling of vascular elements within these lesions. However, the nodular hyperplasia of the involved parenchyma needs to be explained. An observation by Paradis *et al*^[5], using the XCI analysis, revealed polyclonality in all of the 12 FNH lesions examined. However, data from other laboratories, obtained by similar assays, demonstrated monoclonality in FNH lesions at frequencies ranging from 39%^[9] to 75%^[7]. The reason for this discrepancy is currently unknown. Insufficient sampling may result in the occurrence of skewed XCI patterns during a test with

normal tissues^[28,47], which may lead to misinterpretation of the data. The phenomenon was associated with clonal cell clusters (patching) as described in other tissues^[28,47-49]. It may also be true that clonal proliferation occurs focally within some of the classical lesions.

In this study, the neoplastic nature of HCC and HCA was confirmed, however, a random XCI inactivation pattern was demonstrated in all of the eight FNH lesions examined. In order to avoid interference from clonal patches, large samples were analyzed for all the lesions. Our results demonstrate that classical FNH, when examined as a whole, is polyclonal in cell composition. The assay is useful for the differential diagnosis between FNH and neoplastic hepatocellular lesions including HCA and HCC.

Human hepatocarcinogenesis is a multi-step process,

including the occurrence of FAH and NAH, neoplastic formation and malignant transformation through high-grade SCC to a fully developed HCC^[20,22]. The sequential changes may involve inactivation of multiple tumor suppressors^[38]. LOH is one of the main mechanisms for inactivation of tumor suppressor genes. Its occurrence has been localized frequently at 1p, 6q, 8p, 11p and 16q in early-stage, small HCC, while the losses at 4q, 13q and 17p were linked to progression of the lesion^[30-38]. As some well-differentiated HCCs and HCAs with high-grade SCC share many morphologic features, it may be difficult to make the differential diagnosis between these disorders with full certainty. This is particularly true when the lesion occurs in a liver without chronic viral hepatitis and cirrhosis. Activation of β -catenin and Wnt-1 signaling pathway has been linked to HCA lesions showing various degrees of phenotypes indicative of malignant transformation^[11,14], however, these changes were also found in some HCCs^[50,51]. In this study, we examined the allelic integrity of these chromosomal arms using 57 microsatellite markers in nine HCAs and 18 well-differentiated HCCs. Frequent LOH was observed in these well-differentiated HCCs at loci on 6q, 8p, 11p, 16q and 17p. In HCAs, the alterations were observed on similar chromosomal arms, but at different loci (Figure 5). Among the eight loci selected for 8p, four showed LOH, located at D8S261, D8S1754, D8S277 and D8S298, in HCC, and only one in HCA, at D8S298. Among the seven loci for 16q, four showed LOH in HCC, located at D16S3029, D16S303, D16S3040 and D16S402, and only one, at D16S303, in HCA. It seems that the demonstration of 8p losses at D8S261, D8S1754 and D8S277, 16q losses at D16S3029 and D16S3040, and 17p loss at 17S796 is helpful for the identification of HCC from HCA.

In contrast to HCA, FNH did not show TCF1/HNF-1 α or CTNNB1 gene mutations and rarely showed DNA losses^[14,52,53]. Allelic imbalances are also present in the majority of HCAs, as shown in this study, but results of LOH detection in FNH are confusing. A genome-wide assay by Bioulac-Sage and colleagues demonstrated LOH in 5 (26%) of the 19 classical FNH samples^[9], but another group, using a similar approach, did not find any LOH among the 212 informative loci^[54]. In the present study, we did not find LOH at any of the 57 loci in the six FNH lesions, as tested using samples as large as 1 cm \times 1 cm. This is consistent to the polyclonal nature of FNH as revealed in most of the lesions.

Results from our previous studies on human liver has enabled us to identify FAH and NAH in both explanted and resected liver specimens, and these lesions were associated with SCC and a markedly increased risk of HCC development^[20,22]. In a recent study, various kinds of nodules from livers with HBV-associated cirrhosis were microdissected. XCI assay revealed monoclonality in all of the NAH with SCC, 35% of the NAH without SCC, but not in any of the ordinary regenerative nodules examined^[27]. These NAH with clonal expansion were considered neoplastic, designated microadenomas and

representing hepatic intraepithelial neoplasia (HIN). In this study, multiple FAH and NAH were also identified in FNH lesions, all of these lesions were composed mainly of clear hepatocytes with none showing SCC. A total of 56 NAH were isolated from four FNH lesions, and monoclonality was revealed in 21 (40%) of the 52 informative NAH by XCI analysis, demonstrating multifocal microadenoma formation within FNH. In contrast, all of the five ordinary nodules were proven to be polyclonal.

The occurrence of NAH with different inactivation patterns, as shown in FNH09 (Figure 3B and C), proves that microadenomas develop independently, as described for multiple leiomyomas of the uterus^[28]. It is conceivable that FNH is composed of numerous NAH and NAH-forming lesions. The synchronous relationship between different NAH may provide an explanation for the stable behavior of most FNH lesions, in contrast to HCA. In addition, the presence of multiple microadenomas (HIN) with similar XCI patterns in an FNH lesion, as shown in FNH11 (Figure 3D), may result in misinterpretation of the data if the sample examined is small. For this reason, we proposed that sample areas for clonality assessment should be as large as 1 cm \times 1 cm for larger FNH or cover the largest cross section for smaller lesions.

While some NAH were shown to be monoclonal, their pathogenesis is unknown. Our assay demonstrated allelic imbalance in all of the 13 lesions, providing additional evidence for their neoplastic nature. The alterations were highly frequent in six loci, involving similar chromosomal arms, as in HCA, including 8p, 11p, 13q and 17p. However, chromosomal arms 8p and 16q were affected in different frequencies in these two types of lesions. D8S298 was affected frequently in both NAH and HCAs, but LOH at this locus was revealed in only a minority of the HCC lesions. Allelic imbalance at D8S298 has been observed in oral and laryngeal squamous cell carcinoma and its precursor lesions. The change was proposed to be an early event in development of the cancer^[55]. This change was also observed in HCC specimens, with its frequencies ranging from 15%^[56] to 32%^[57]. It remains to be determined whether there is a tumor suppressor gene near D8S298 preferentially responsible for HCC development in HBsAg-negative patients.

In summary, classical FNH lesions were shown to be polyclonal by XCI and LOH assays and distinguishable from HCA and HCC. Secondly, multifocal HIN formation, in the form of NAH, was demonstrated within the FNH lesions. In addition, allelic imbalances were also identified in the microdissected NAH, with similar chromosomal arms affected as in HCAs. Therefore, classical FNH is considered a cluster of NAH. Elucidation of the process will be helpful for further understanding of early human hepatocarcinogenesis.

ACKNOWLEDGMENTS

The authors thank Dr. Lin Yang for her statistical assistance, Professor Peter Bannasch and Yan-Fang Liu for helpful

discussions, Dr. Su-Sheng Shi for providing valuable tissue samples, Xiu-Yun Liu, Xin-Hua Xue and Yong-Qiang Xie for their technical assistance.

COMMENTS

Background

Focal nodular hyperplasia (FNH) is a lesion found in an otherwise normal liver, and is considered parenchyma overgrowth responsive to increased blood flow secondary to vascular malformations. While its clinical outcomes are believed to be different from hepatocellular adenoma (HCA) and carcinoma, its pathogenesis is largely unclear and its distinction from HCA is sometimes difficult.

Research frontiers

While FNH was proposed to be a hyperplastic lesion, its clonality status has not been elucidated and the development of hepatocyte nodules within the involved parenchyma needs to be explained. In this study, the authors demonstrate that classical FNH, when examined as a whole, is polyclonal in cell composition. However, the formation of multiple nodules of altered hepatocytes (NAH), showing monoclonality and genetic alterations, was found within all the FNH lesions.

Innovations and breakthroughs

Clonality status of FNH has not been clarified and the mechanism for development of multiple hepatocyte nodules within FNH is unknown. In this study, classical FNH lesions were shown to be polyclonal and distinguishable from HCA and carcinoma. Secondly, the multifocal formation of NAH, representing early-stage hepatic intraepithelial neoplasia (HIN), was demonstrated within the FNH lesions. In addition, allelic imbalances were also identified in microdissected NAH. Classical FNH is considered a cluster of NAH.

Applications

The results of clonality analyses demonstrated polyclonality in all the classical FNH lesions, the approach being useful for the differential diagnosis of FNH from HCA and well-differentiated carcinoma. In addition, elucidation of the pathogenesis of the NAH lesions, representing hepatocytic microadenoma and early-stage HIN, may lead to further understanding of early human hepatocarcinogenesis.

Terminology

Most, if not all, of HCAs and carcinomas develop from a single focus of altered hepatocytes through nodular transformation (formation of NAH) and appearance of cellular and architectural atypia (small-cell change). Monoclonality and nonrandom genetic alterations similar to HCA, as demonstrated in NAH lesions in this study, enable us to consider these lesions hepatocytic microadenoma that represent early-stage HIN.

Peer review

This is an interesting report of clonality and genetic alternations in FNH. The article is well written and deserves publishing.

REFERENCES

- Hirohashi S, Ishak KG, Kojiro M, Wanless IR, Theise ND, Tsukuma H, Blum HE, Deugnier Y, Laurent Puig P, Fischer HP, Sakamoto M. Hepatocellular carcinoma. In: Aaltonen LA, Hamilton SR, editors. Pathology and genetics of tumors of the digestive system. Lyon: IARC Press, 2000: 159-172
- Anthony PP. Tumors and tumor-like lesions of the liver and biliary tract: etiology, epidemiology and pathology. In: MacSween RNM, Burt AD, Portmann BC, Ishak KG, Scheuer PJ, Anthony PP, editors. Pathology of the liver. 4th ed. London: Churchill Livingstone, 2002: 711-776
- Wanless IR, Mawdsley C, Adams R. On the pathogenesis of focal nodular hyperplasia of the liver. *Hepatology* 1985; **5**: 1194-1200
- Nguyen BN, Fléjou JF, Terris B, Belghiti J, Degott C. Focal nodular hyperplasia of the liver: a comprehensive pathologic study of 305 lesions and recognition of new histologic forms. *Am J Surg Pathol* 1999; **23**: 1441-1454
- Paradis V, Laurent A, Flejou JF, Vidaud M, Bedossa P. Evidence for the polyclonal nature of focal nodular hyperplasia of the liver by the study of X-chromosome inactivation. *Hepatology* 1997; **26**: 891-895
- Gong L, Su Q, Zhang W, Li AN, Zhu SJ, Feng YM. Liver cell adenoma: a case report with clonal analysis and literature review. *World J Gastroenterol* 2006; **12**: 2125-2129
- Gaffey MJ, Iezzoni JC, Weiss LM. Clonal analysis of focal nodular hyperplasia of the liver. *Am J Pathol* 1996; **148**: 1089-1096
- Paradis V, Benzekri A, Dargère D, Bièche I, Laurendeau I, Vilgrain V, Belghiti J, Vidaud M, Degott C, Bedossa P. Telangiectatic focal nodular hyperplasia: a variant of hepatocellular adenoma. *Gastroenterology* 2004; **126**: 1323-1329
- Bioulac-Sage P, Rebouissou S, Sa Cunha A, Jeannot E, Lepreux S, Blanc JF, Blanché H, Le Bail B, Saric J, Laurent-Puig P, Balabaud C, Zucman-Rossi J. Clinical, morphologic, and molecular features defining so-called telangiectatic focal nodular hyperplasias of the liver. *Gastroenterology* 2005; **128**: 1211-1218
- Edmondson HA. Differential diagnosis of tumors and tumor-like lesions of liver in infancy and childhood. *AMA J Dis Child* 1956; **91**: 168-186
- Rebouissou S, Bioulac-Sage P, Zucman-Rossi J. Molecular pathogenesis of focal nodular hyperplasia and hepatocellular adenoma. *J Hepatol* 2008; **48**: 163-170
- Ishak KG. Hepatic lesions caused by anabolic and contraceptive steroids. *Semin Liver Dis* 1981; **1**: 116-128
- Bannasch P, Schröder CH. Tumors and tumor-like lesions of the liver and biliary tract: pathogenesis of primary liver tumors. In: MacSween RNM, Burt AD, Portmann BC, Ishak KG, Scheuer PJ, Anthony PP, editors. Pathology of the liver. 4th ed. London: Churchill Livingstone, 2002: 777-825
- Zucman-Rossi J, Jeannot E, Nhieu JT, Scoazec JY, Guettier C, Rebouissou S, Bacq Y, Leteurtre E, Paradis V, Michalak S, Wendum D, Chiche L, Fabre M, Mellottee L, Laurent C, Partensky C, Castaing D, Zafrani ES, Laurent-Puig P, Balabaud C, Bioulac-Sage P. Genotype-phenotype correlation in hepatocellular adenoma: new classification and relationship with HCC. *Hepatology* 2006; **43**: 515-524
- Bannasch P, Jahn U-R, Hacker HJ, Su Q, Hofmann W, Pichlmayr R, Otto G. Focal hepatic glycogenosis: a putative preneoplastic lesion associated with neoplasia and cirrhosis in explanted human livers. *Int J Oncol* 1997; **10**: 261-268
- Chen TC, Chou TB, Ng KF, Hsieh LL, Chou YH. Hepatocellular carcinoma associated with focal nodular hyperplasia. Report of a case with clonal analysis. *Virchows Arch* 2001; **438**: 408-411
- Kellner U, Jacobsen A, Kellner A, Mantke R, Roessner A, Röcken C. Comparative genomic hybridization. Synchronous occurrence of focal nodular hyperplasia and hepatocellular carcinoma in the same liver is not based on common chromosomal aberrations. *Am J Clin Pathol* 2003; **119**: 265-271
- Petsas T, Tsamandas A, Tsota I, Karavias D, Karatza C, Vassiliou V, Kardamakis D. A case of hepatocellular carcinoma arising within large focal nodular hyperplasia with review of the literature. *World J Gastroenterol* 2006; **12**: 6567-6571
- Shen YH, Fan J, Wu ZQ, Ma ZC, Zhou XD, Zhou J, Qiu SJ, Qin LX, Ye QH, Sun HC, Huang XW, Tang ZY. Focal nodular hyperplasia of the liver in 86 patients. *Hepatobiliary Pancreat Dis Int* 2007; **6**: 52-57
- Su Q, Benner A, Hofmann WJ, Otto G, Pichlmayr R, Bannasch P. Human hepatic preneoplasia: phenotypes and proliferation kinetics of foci and nodules of altered hepatocytes and their relationship to liver cell dysplasia. *Virchows Arch* 1997; **431**: 391-406
- Su Q, Zerban H, Otto G, Bannasch P. Cytokeratin expression is reduced in glycogenotic clear hepatocytes but increased in ground-glass cells in chronic human and woodchuck hepadnaviral infection. *Hepatology* 1998; **28**: 347-359
- Su Q, Bannasch P. Relevance of hepatic preneoplasia for human hepatocarcinogenesis. *Toxicol Pathol* 2003; **31**: 126-133

- 23 **Watanabe S**, Okita K, Harada T, Kodama T, Numa Y, Takemoto T, Takahashi T. Morphologic studies of the liver cell dysplasia. *Cancer* 1983; **51**: 2197-2205
- 24 **Edmondson HA**, Steiner PE. Primary carcinoma of the liver: a study of 100 cases among 48,900 necropsies. *Cancer* 1954; **7**: 462-503
- 25 **Su Q**, Schröder CH, Otto G, Bannasch P. Overexpression of p53 protein is not directly related to hepatitis B x protein expression and is associated with neoplastic progression in hepatocellular carcinomas rather than hepatic preneoplasia. *Mutat Res* 2000; **462**: 365-380
- 26 **Noguchi S**, Motomura K, Inaji H, Imaoka S, Koyama H. Clonal analysis of human breast cancer by means of the polymerase chain reaction. *Cancer Res* 1992; **52**: 6594-6597
- 27 **Chu X**, Su Q, Gong L, Zhang W, Wang SF, Zhu SJ, Li AN, Feng YM. Clonality of nodules of altered hepatocytes in livers with chronic hepatitis B and cirrhosis. *Shijie Huaren Xiaohua Zazhi* 2005; **13**: 945-952
- 28 **Cai YR**, Diao XL, Wang SF, Zhang W, Zhang HT, Su Q. X-chromosomal inactivation analysis of uterine leiomyomas reveals a common clonal origin of different tumor nodules in some multiple leiomyomas. *Int J Oncol* 2007; **31**: 1379-1389
- 29 **Garcia SB**, Novelli M, Wright NA. The clonal origin and clonal evolution of epithelial tumours. *Int J Exp Pathol* 2000; **81**: 89-116
- 30 **Lin YW**, Sheu JC, Liu LY, Chen CH, Lee HS, Huang GT, Wang JT, Lee PH, Lu FJ. Loss of heterozygosity at chromosome 13q in hepatocellular carcinoma: identification of three independent regions. *Eur J Cancer* 1999; **35**: 1730-1734
- 31 **Bando K**, Nagai H, Matsumoto S, Koyama M, Kawamura N, Tajiri T, Onda M, Emi M. Identification of a 1-Mb common region at 16q24.1-24.2 deleted in hepatocellular carcinoma. *Genes Chromosomes Cancer* 2000; **28**: 38-44
- 32 **Kondo Y**, Kanai Y, Sakamoto M, Mizokami M, Ueda R, Hirohashi S. Genetic instability and aberrant DNA methylation in chronic hepatitis and cirrhosis--A comprehensive study of loss of heterozygosity and microsatellite instability at 39 loci and DNA hypermethylation on 8 CpG islands in microdissected specimens from patients with hepatocellular carcinoma. *Hepatology* 2000; **32**: 970-979
- 33 **Sun M**, Eshleman JR, Ferrell LD, Jacobs G, Sudilovsky EC, Tuthill R, Hussein MR, Sudilovsky O. An early lesion in hepatic carcinogenesis: loss of heterozygosity in human cirrhotic livers and dysplastic nodules at the 1p36-p34 region. *Hepatology* 2001; **33**: 1415-1424
- 34 **Chan KL**, Lee JM, Guan XY, Fan ST, Ng IO. High-density allelotyping of chromosome 8p in hepatocellular carcinoma and clinicopathologic correlation. *Cancer* 2002; **94**: 3179-3185
- 35 **Wong CM**, Lee JM, Lau TC, Fan ST, Ng IO. Clinicopathological significance of loss of heterozygosity on chromosome 13q in hepatocellular carcinoma. *Clin Cancer Res* 2002; **8**: 2266-2272
- 36 **Kahng YS**, Lee YS, Kim BK, Park WS, Lee JY, Kang CS. Loss of heterozygosity of chromosome 8p and 11p in the dysplastic nodule and hepatocellular carcinoma. *J Gastroenterol Hepatol* 2003; **18**: 430-436
- 37 **Zhang SH**, Cong WM, Xian ZH, Wu MC. Clinicopathological significance of loss of heterozygosity and microsatellite instability in hepatocellular carcinoma in China. *World J Gastroenterol* 2005; **11**: 3034-3039
- 38 **Lee JM**, Wong CM, Ng IO. Hepatitis B virus-associated multistep hepatocarcinogenesis: a stepwise increase in allelic alterations. *Cancer Res* 2008; **68**: 5988-5996
- 39 **Henegariu O**, Heerema NA, Dlouhy SR, Vance GH, Vogt PH. Multiplex PCR: critical parameters and step-by-step protocol. *Biotechniques* 1997; **23**: 504-511
- 40 **Heinemann LA**, Weimann A, Gerken G, Thiel C, Schlaud M, DoMinh T. Modern oral contraceptive use and benign liver tumors: the German Benign Liver Tumor Case-Control Study. *Eur J Contracept Reprod Health Care* 1998; **3**: 194-200
- 41 **Mathieu D**, Kobeiter H, Maison P, Rahmouni A, Cherqui D, Zafrani ES, Dhumeaux D. Oral contraceptive use and focal nodular hyperplasia of the liver. *Gastroenterology* 2000; **118**: 560-564
- 42 **Côté C**. Regression of focal nodular hyperplasia of the liver after oral contraceptive discontinuation. *Clin Nucl Med* 1997; **22**: 587-590
- 43 **Ohmoto K**, Honda T, Hirokawa M, Mitsui Y, Iguchi Y, Kuboki M, Yamamoto S. Spontaneous regression of focal nodular hyperplasia of the liver. *J Gastroenterol* 2002; **37**: 849-853
- 44 **Scalori A**, Tavani A, Gallus S, La Vecchia C, Colombo M. Oral contraceptives and the risk of focal nodular hyperplasia of the liver: a case-control study. *Am J Obstet Gynecol* 2002; **186**: 195-197
- 45 **Yamamoto M**, Ariizumi S, Yoshitoshi K, Saito A, Nakano M, Takasaki K. Hepatocellular carcinoma with a central scar and a scalloped tumor margin resembling focal nodular hyperplasia in macroscopic appearance. *J Surg Oncol* 2006; **94**: 587-591
- 46 **Paradis V**, Bièche I, Dargère D, Laurendeau I, Nectoux J, Degott C, Belghiti J, Vidaud M, Bedossa P. A quantitative gene expression study suggests a role for angiopoietins in focal nodular hyperplasia. *Gastroenterology* 2003; **124**: 651-659
- 47 **Chung IM**, Schwartz SM, Murry CE. Clonal architecture of normal and atherosclerotic aorta: implications for atherogenesis and vascular development. *Am J Pathol* 1998; **152**: 913-923
- 48 **Guo Z**, Thunberg U, Sallstrom J, Wilander E, Ponten J. Clonality analysis of cervical cancer on microdissected archival materials by PCR-based X-chromosome inactivation approach. *Int J Oncol* 1998; **12**: 1327-1332
- 49 **Diallo R**, Schaefer KL, Poremba C, Shivazi N, Willmann V, Buerger H, Dockhorn-Dworniczak B, Boecker W. Monoclonality in normal epithelium and in hyperplastic and neoplastic lesions of the breast. *J Pathol* 2001; **193**: 27-32
- 50 **de La Coste A**, Romagnolo B, Billuart P, Renard CA, Buendia MA, Soubrane O, Fabre M, Chelly J, Beldjord C, Kahn A, Perret C. Somatic mutations of the beta-catenin gene are frequent in mouse and human hepatocellular carcinomas. *Proc Natl Acad Sci USA* 1998; **95**: 8847-8851
- 51 **Laurent-Puig P**, Zucman-Rossi J. Genetics of hepatocellular tumors. *Oncogene* 2006; **25**: 3778-3786
- 52 **Chen YJ**, Chen PJ, Lee MC, Yeh SH, Hsu MT, Lin CH. Chromosomal analysis of hepatic adenoma and focal nodular hyperplasia by comparative genomic hybridization. *Genes Chromosomes Cancer* 2002; **35**: 138-143
- 53 **Chen YW**, Jeng YM, Yeh SH, Chen PJ. P53 gene and Wnt signaling in benign neoplasms: beta-catenin mutations in hepatic adenoma but not in focal nodular hyperplasia. *Hepatology* 2002; **36**: 927-935
- 54 **Nakayama S**, Kanbara Y, Nishimura T, Nishida N, Hanioka K, Morita M, Fujita M, Sakurai K, Hayashi Y. Genome-wide microsatellite analysis of focal nodular hyperplasia: a strong tool for the differential diagnosis of non-neoplastic liver nodule from hepatocellular carcinoma. *J Hepatobiliary Pancreat Surg* 2006; **13**: 416-420
- 55 **El-Naggar AK**, Coombes MM, Batsakis JG, Hong WK, Goepfert H, Kagan J. Localization of chromosome 8p regions involved in early tumorigenesis of oral and laryngeal squamous carcinoma. *Oncogene* 1998; **16**: 2983-2987
- 56 **Lu T**, Hano H, Meng C, Nagatsuma K, Chiba S, Ikegami M. Frequent loss of heterozygosity in two distinct regions, 8p23.1 and 8p22, in hepatocellular carcinoma. *World J Gastroenterol* 2007; **13**: 1090-1097
- 57 **Pang JZ**, Qin LX, Ren N, Hei ZY, Ye QH, Jia WD, Sun BS, Lin GL, Liu DY, Liu YK, Tang ZY. Loss of heterozygosity at D8S298 is a predictor for long-term survival of patients with tumor-node-metastasis stage I of hepatocellular carcinoma. *Clin Cancer Res* 2007; **13**: 7363-7369